Supplementary Material: Low cost bimetallic $AuCu_3$ tetramer on Ti_2CO_2 MXene as an efficient catalyst for CO oxidation: A theoretical prediction

Aswathi Mohan T[1, a)] and Prasenjit Ghosh[2, b)]

[1)] *Department of Chemistry, Indian Institute of Science Education and Research (IISER), Pune 411008, Maharashtra , India*

[2)] *Department of Physics, Centre for Energy Science, Indian Institute of Science Education and Research (IISER), Pune 411008, Maharashtra , India*

[a)] Electronic mail: aswathi.mohan@students.iiserpune.ac.in

[b)] Electronic mail: pghosh@iiserpune.ac.in

TABLE S1. Adsorption energy of bimetallic clusters on Ti_2CO_2 MXene.

Cluster composition	Adsorption energy (eV)
Cu_4	-3.56
Au_4	-2.08
$AuCu_3$	-3.41
Au_2Cu_2	-2.23
Au_3Cu	-2.31

TABLE S2. Adsorption energy of CO and O_2 on $AuCu_3/Ti_2CO_2$.

Species	Adsorption energy (eV)
CO	-1.26
O_2	-0.83
CO + O_2	-2.16

MvK mechanism: A crucial factor decisive of this path is oxygen vacancy formation energy. For Ti_2CO_2, it was found to be 3.27 eV[1], which is comparable to substrates like rutile TiO_2(110) (around 3.00 eV) that is known for facile oxygen vacancy formation[2]. Hence to investigate the MvK mechanism for CO oxidation, we take the most stable CO adsorption geometry (**IS4** in Fig. S3). From the reaction thermodynamic studies, we find that CO attacks an O atom from the top layer of Ti_2CO_2, forming a CO_2 intermediate (**INT12**), 2.23 eV higher in energy. The next step of CO_2 desorption is also endothermic, making the whole mechanism unlikely to happen.

TABLE S3. Reaction barrier for CO oxidation on $AuCu_3/Ti_2CO_2$.

Cycle	Mechanism	Reaction barrier (eV)
First	LH	0.56
Second	ER	0.37
Second	LH	0.57

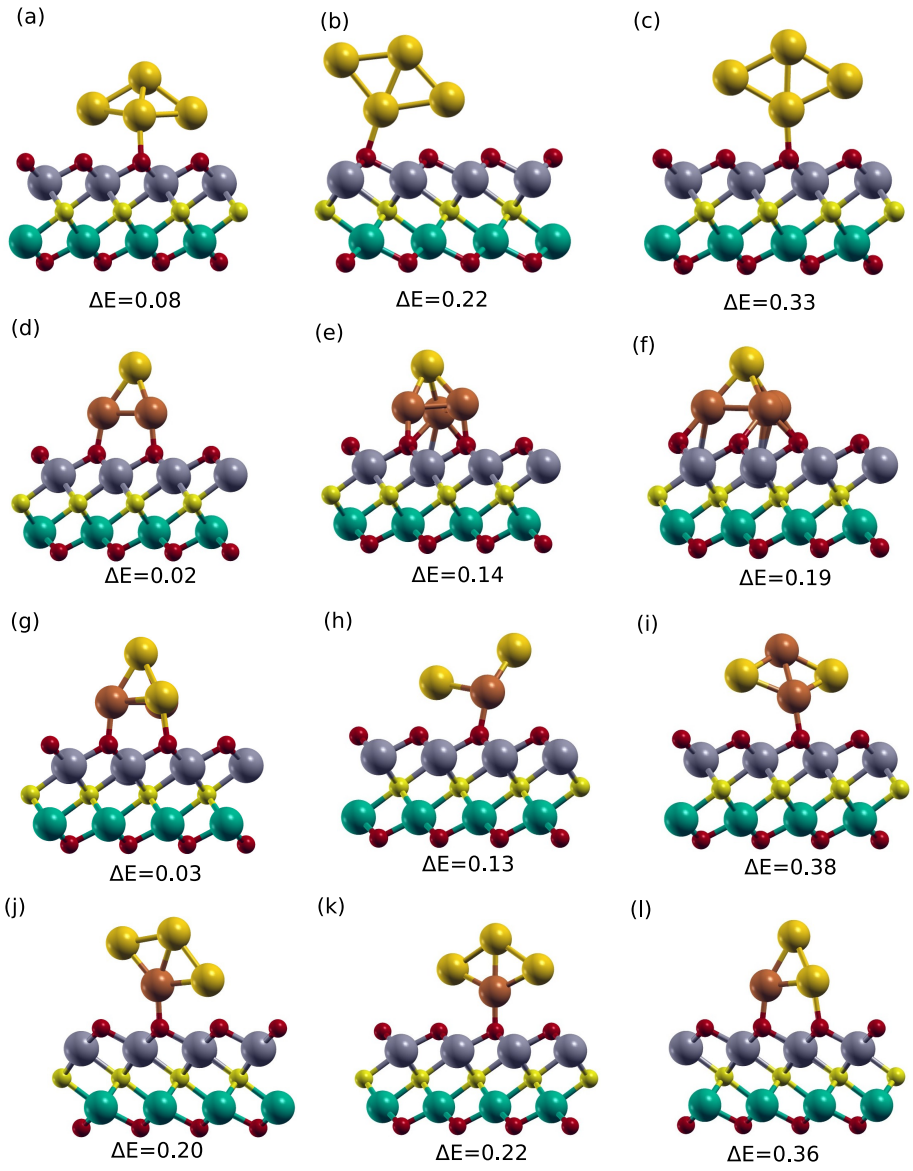

FIG. S1. Stable higher energy structures of a)-c) Au_4, d)-f) $AuCu_3$, g)-i) Au_2Cu_2 and j)-l) Au_3Cu clusters deposited on Ti_2CO_2 MXene. Relative energy with respect to the corresponding most stable geometry given in eV.

REFERENCES

[1]L. Xiao-Hong, S. Xiang-Ying and Z. Rui-Zhou, *RSC advances*, 2019, **9**, 27646–27651.

[2]M. V. Ganduglia-Pirovano, A. Hofmann and J. Sauer, *Surface science reports*, 2007, **62**, 219–270.

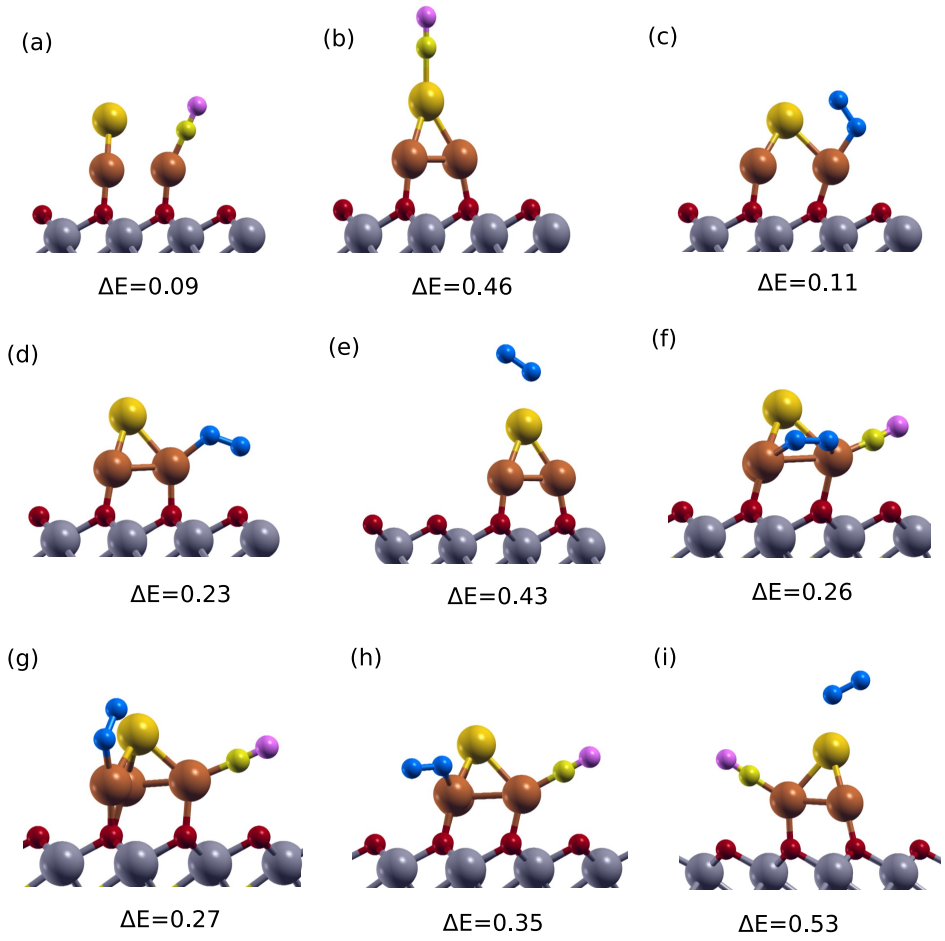

FIG. S2. Stable higher energy structures of a)-b) CO, c)-e) O_2 and f)-i) CO and O_2 co-adsorption on $AuCu_3/Ti_2CO_2$. Relative energy with respect to the corresponding most stable geometry given in eV.

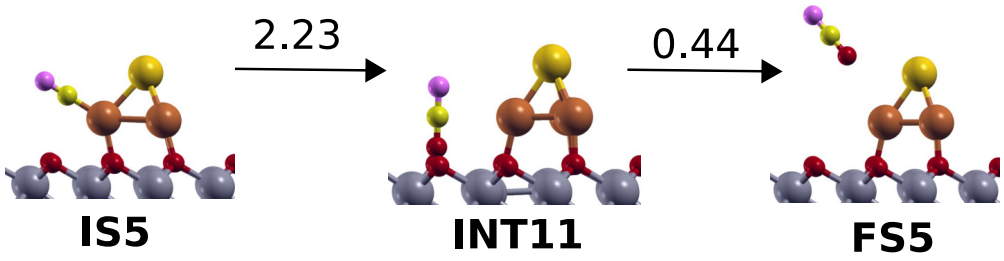

FIG. S3. First cycle of CO oxidation via MvK mechanism on $AuCu_3/Ti_2CO_2$. The reaction energies in eV are marked above the arrow for each step.

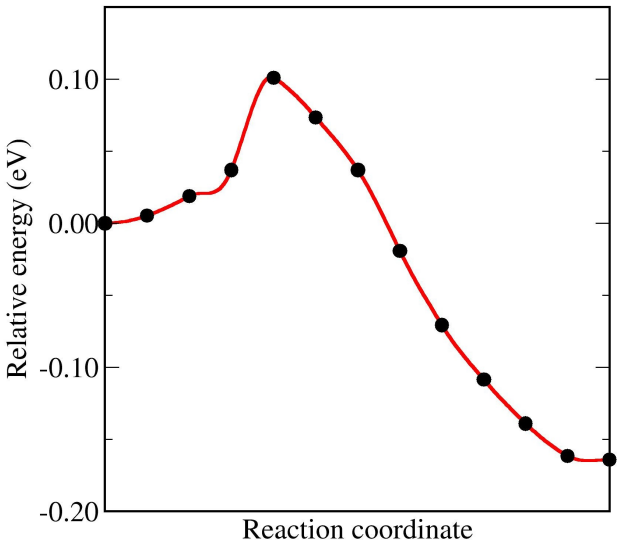

FIG. S4. Reaction energy profile of **IS1** to **INT1**.

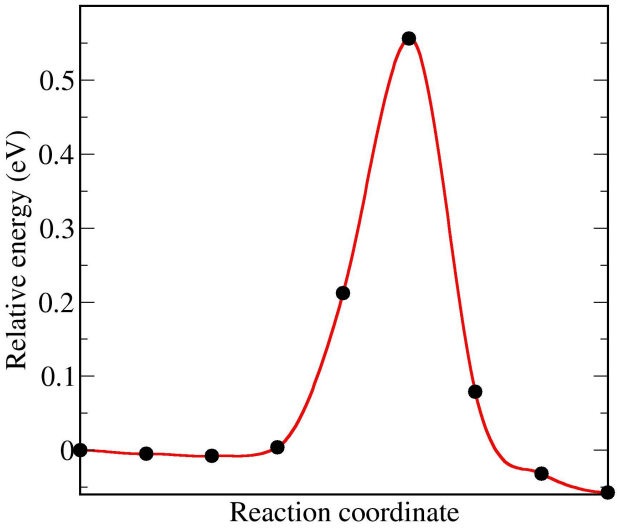

FIG. S5. Reaction energy profile of **INT1** to **INT2**.

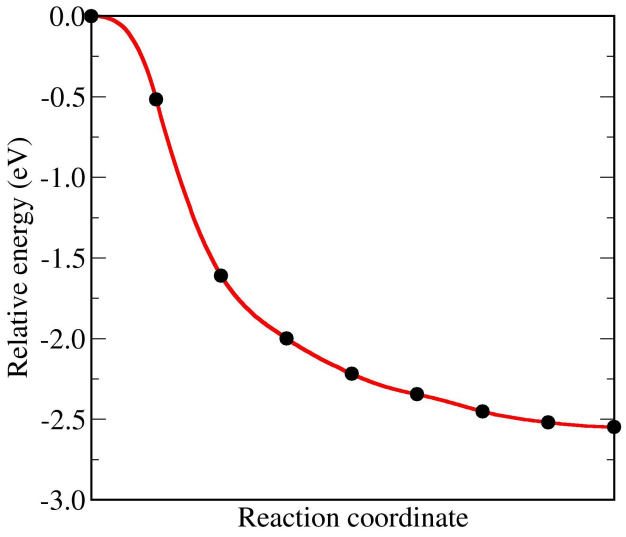

FIG. S6. Reaction energy profile of **INT2** to **INT3**.

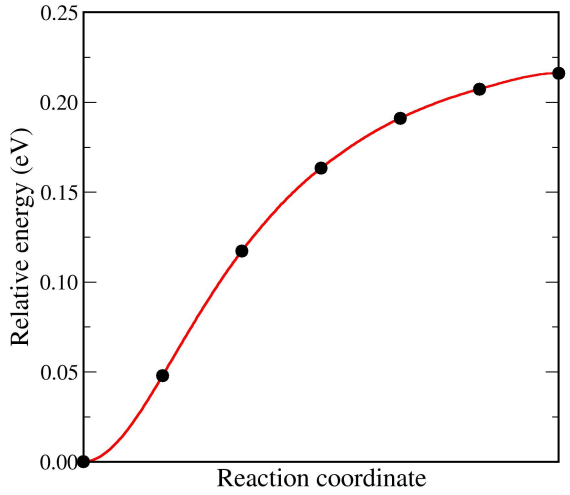

FIG. S7. Reaction energy profile of **INT3** to **FS1**.

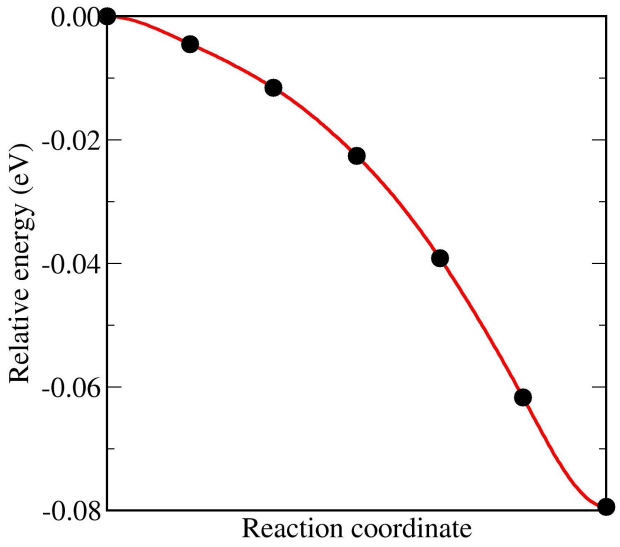

FIG. S8. Reaction energy profile of **IS2** to **INT4**.

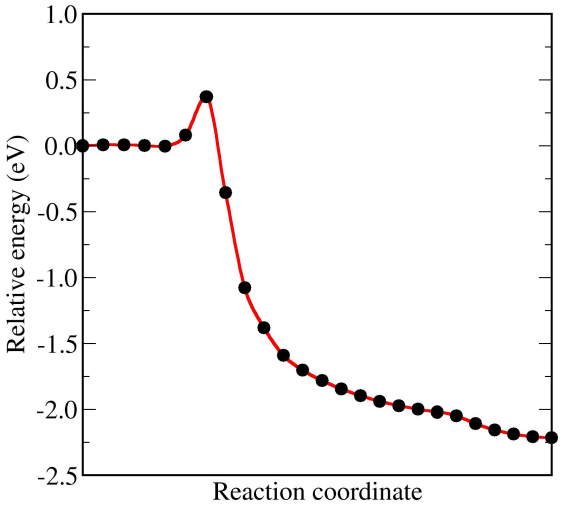

FIG. S9. Reaction energy profile of **INT4** to **INT5**.

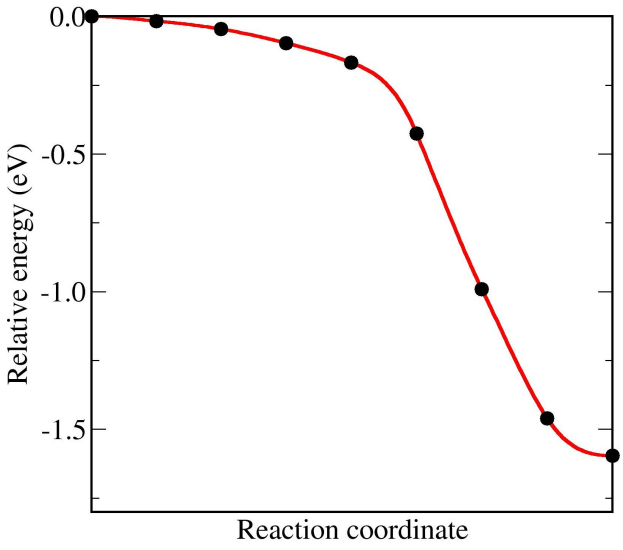

FIG. S10. Reaction energy profile of **INT4** to **INT5**.

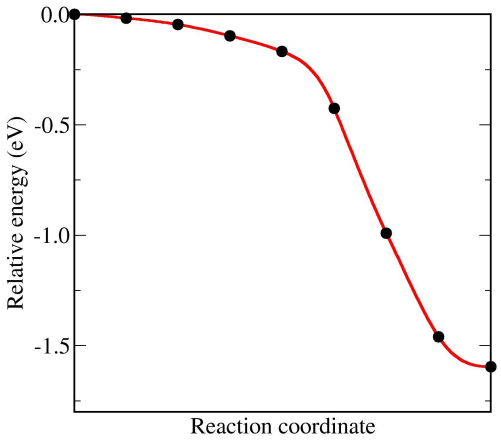

FIG. S11. Reaction energy profile of **IS3** to **INT7**.

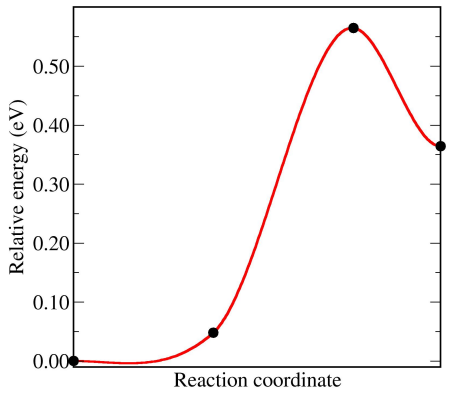

FIG. S12. Reaction energy profile of **INT7** to **INT8**.

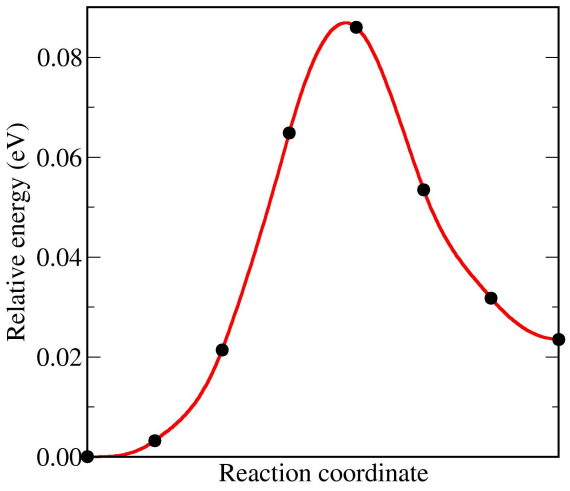

FIG. S13. Reaction energy profile of **INT8** to **INT9**.

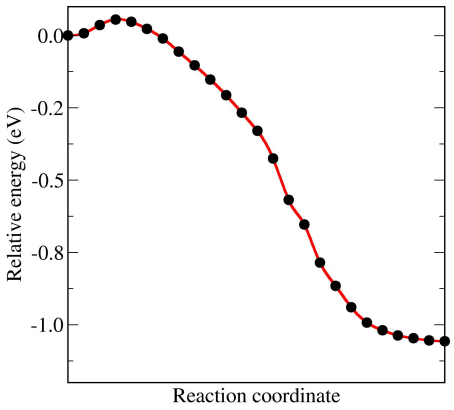

FIG. S14. Reaction energy profile of **INT9** to **INT10**.

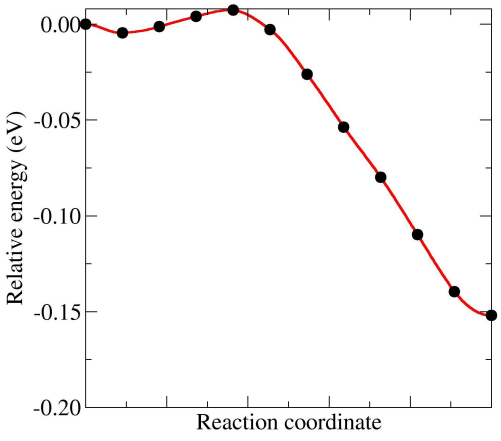

FIG. S15. Reaction energy profile of **INT10** to **INT11**.

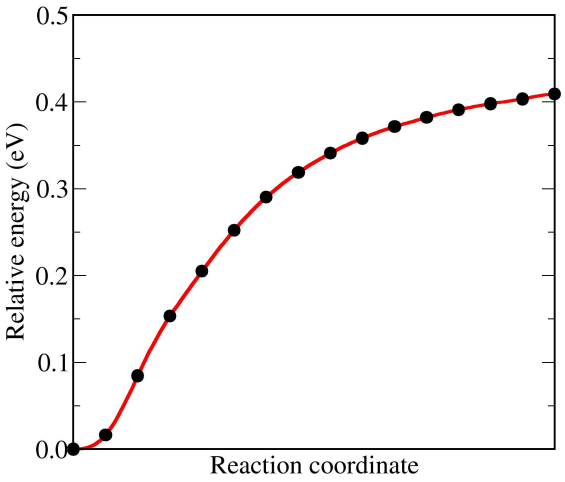

FIG. S16. Reaction energy profile of **INT11** to **FS3**.